ISSN: 3064-6758 www.aristonpubs.com/sciengg-advances https://doi.org/10.69626/sea.2024.0087

RESEARCH ARTICLE

Generating Sub–Wavelength Longitudinal Magnetization Chains using High NA Lens System

M. Udhayakumar [1], P. Raju [1], S. Aswanth [2], K.B. Rajesh [2,*]

ABSTRACT: This study investigates the light-induced magnetization distribution produced by a closely focused, azimuthally polarized Laguerre-Bessel-Gaussian beam, which is superimposed with a helical phase and modulated by an optimized multi-belt complex phase filter (MBCPF). Utilizing vector diffraction theory and the inverse Faraday Effect, we numerically analyze the resulting magnetization patterns. Our findings reveal that by adjusting the radii of the complex phase filter's rings, various novel magnetization focal distributions can be achieved. These include the formation of multiple sub-wavelength spherical magnetization spots arranged in chains of two, three, five, and seven. These configurations are particularly suitable for applications such as transporting multiple magnetic particles, storing multilayer magneto-optical data, developing ultra-compact optomagnetic devices, and fabricating magnetic lattices for spin wave operations.

Keywords: Vector diffraction theory, Inverse Faraday Effect (IFE), Laguerre-Bessel-Gaussian beam, Multiple optical trapping.

Received: 07 March 2024; Revised: 28 April 2024; Accepted: 29 May 2024; Available Online: 13 June 2024

1. INTRODUCTION

Research into atomic field and magneto-optical materials has gained significant traction in recent years due to their intriguing properties and potential applications in fields such as atomic trapping, confocal microscopy, and all-optical magnetic recording (AOMR) [1-4]. These applications benefit from precise control over magnetic fields at subwavelength scales, which can significantly enhance the resolution and efficiency of various technologies. In AOMR, for example, focusing a circularly polarized beam with a high numerical aperture (NA) to produce light-induced subwavelength magnetic spots has proven effective for longitudinal magnetization recording [5-7]. However, the presence of a transverse magnetization component, often with a hollow shape, can degrade the quality of optical magnetic recordings [8–10]. Therefore, generating a pure longitudinal magnetization field has become a critical focus of recent research.

One promising approach involves the use of azimuthally polarized beams. Jiang et al. [11] studied the suppression of transverse magnetization fields by tightly focusing an azimuthally polarized vortex beam, which showed effective suppression of unwanted transverse components. Building on this, Wang et al. [12] achieved a longitudinal magnetization needle with an ultralong longitudinal depth of 7.48λ and a subwavelength lateral size of 0.38λ by using an annular vortex binary filter. This configuration allowed for precise control over the magnetization field, enhancing the longitudinal component while minimizing the transverse one. Ma et al. [13] further advanced this technique by developing an annular phase filter specifically tailored for azimuthally polarized vortex beams. They achieved a pure longitudinal magnetization needle with a remarkable depth of 28λ and a lateral dimension of 0.27λ, showcasing the potential for highly refined magnetization control.

In addition to these advancements, Z. Nie et al. [14-15] proposed a novel method for generating sub-wavelength pure

[1] Department of Physics VSB College of Engineering Technical Campus, Coimbatore, Tamilnadu, India
[2] Department of Physics, Chikkanna Government Arts College, Tiruppur, Tamilnadu, India

* Author to whom correspondence should be addressed: udhayaphy1985@gmail.com (M. Udhayakumar)

longitudinal magnetization chains in the focal region. By tightly focusing an azimuthally polarized Bessel-Gaussian (BG) beam phase modulated by specially designed vortex binary filters and using radially polarized vortex beams under 4Pi focusing, they were able to create a series of magnetization spots with subwavelength precision. This method allowed for the generation of a magnetization chain with significant potential for various applications in magnetic particle manipulation and high-density data storage.

Expanding on Nie's work, Liping Gong et al. [16] demonstrated that by adjusting the phase difference between two counter-propagating azimuthally polarized vortex beams in a 4Pi system, the movement of the magnetization field along the optical axis could be flexibly controlled. This setup enabled the creation of a super-long (16λ) magnetization chain composed of 19 subwavelength (0.44λ) longitudinal magnetization fields within the focal volume. This innovative approach highlighted the feasibility of generating extended magnetization structures with precise control over their spatial properties.

In this study, we propose a novel method for generating an ultra-long focal depth subwavelength pure longitudinal magnetic probe. Our approach utilizes an azimuthally polarized Laguerre-Bessel-Gaussian (LBG) beam modulated by specially designed complex phase filters. The LBG beam, known for its unique propagation characteristics and ability to maintain its shape over long distances, is ideal for creating extended magnetization structures. By optimizing the design of the complex phase filters, we can achieve multiple magnetic spots with high precision and control.

The numerical analysis, conducted using vector diffraction theory and the inverse Faraday Effect, reveals that varying the radii of the complex phase filter's rings can produce numerous novel magnetization focal distributions. These include the formation of multiple magnetization chains with two, three, five, and seven subwavelength spherical magnetization spots. Such configurations are suitable for transporting multiple magnetic particles, storing multilayer magneto-optical data, developing ultra-compact optomagnetic devices, and fabricating magnetic lattices for spin wave operations.

The implications of this research are significant for the fields of high-resolution magnetic recording, particle manipulation, and the development of advanced magneto-optical devices. The ability to generate and control subwavelength magnetization fields with high precision opens up new possibilities for enhancing the performance and capabilities of various technologies. By leveraging the unique properties of LBG beams and complex phase filters, we can push the boundaries of what is achievable in magneto-optical material research and its practical applications.

This study presents a comprehensive approach to generating ultra-long focal depth subwavelength pure longitudinal magnetic probes and multiple magnetic spots using azimuthally polarized LBG beams. This method holds promise for advancing the precision and effectiveness of magnetization field generation, offering new opportunities for high-precision magnetic recording, manipulation, and the development of innovative optomagnetic devices.

2. THEORY

Figure 1 exhibits a schematic setup to generate the sub-wavelength longitudinal magnetization chain for azimuthally polarized Laguerre–Bessel–Gaussian beam. When an incident Laguerre-Bessel-Gaussian beam is azimuthally polarized, it passes through the spiral phase plate (SPP) and transforms into an LBG beam. The SPP is a type of phase encoding element that, at the beam cross section, delays the incident beam's phase from 0 to 2π along the angular direction. The incident beam through the filter at the back aperture of the objective can be expressed as [17, 18]:

$$T(\theta)=\beta^2\frac{\sin\theta}{\sin^2\alpha}L_p^1\left[\left(\frac{2\beta^2\sin^2\theta}{\sin\alpha}\right)^2\right]J_1\left(2\beta\frac{\sin\theta}{\sin\alpha}\right)\times\exp\left(\frac{-\beta^2\sin^2\theta}{\sin^2\alpha}\right)\rightarrow(1)$$

According to the Richards and Wolf diffraction theory [18-19], the electric field distribution in the focal region can be expressed as:

$$E(r,\varphi,z)=\begin{bmatrix}E_r\\E_\varphi\\E_z\end{bmatrix}=Ai^m\int_0^\alpha T(\varphi)\begin{bmatrix}V_1\\iV_2\\0\end{bmatrix}T(\theta)A(\theta)\exp^{ikz\cos\theta}\sqrt{\cos\theta}\sin\theta\,\mathrm{d}\theta\,\mathrm{d}\theta\rightarrow(2)$$

Where

$$V_1=J_{m-1}(kr\sin\theta)+J_{m+1}(kr\sin\theta)\rightarrow(3)$$

$$V_2=J_{m-1}(kr\sin\theta)-J_{m+1}(kr\sin\theta)\rightarrow(4)$$

Here, A is the relative amplitude r, φ, and z are the cylindrical coordinates in the focal space. J_0 and J_2 denote Bessel functions of the first kind. Equation (2) is represented in cylindrical vector components and it indicates that the filter transforms a beam with pure azimuthal polarization into a beam with radial and azimuthal polarization components that are essential to obtaining longitudinal magnetization at the focus. Based on the IFE, the magnetization field induced by tightly focusing azimuthally polarized beams with helical phase near the focal point is defined as [15]:

$$M=i\gamma E\times E^*\rightarrow(5)$$

where E is the electric field, E* is its conjugate, and γ is a real constant proportional to the susceptibility of the material [23–25]. By substituting Eqs. (2) – (4) into Eq. (5), the magnetization field can be given by:

$$M_z=2\gamma|A|^2\,\mathrm{Re}(\mathrm{I}_1\bullet I_2)\rightarrow(6)$$

$$I_1 = \int_0^{\alpha} \mathrm{T}(\varphi) V_1 \exp^{ikz\cos\theta} \sqrt{\cos\theta}\sin\theta\,\mathrm{d}\theta \rightarrow (7)$$

$$I_2 = \int_0^{\alpha} \mathrm{T}(\varphi) V_2 \exp^{-ikz\cos\theta} \sqrt{\cos\theta}\sin\theta\,\mathrm{d}\theta \rightarrow (8)$$

As described by Eqs. (8), one can easily conclude that the magnetization field induced by an azimuthally polarized vortex beam with tight focus only has a longitudinal component. Through the utilization of the MO film and the azimuthally polarized beam with vortex phase, we are able to manipulate the magnetization field distribution under close focus. Additionally, we have refined the CPF to produce a series of spherical multiple magnetization spots for multiple magnetic particle trapping. The phase and amplitude function *A(θ)* of the MBCPF is given by [26]:

$$MBCPF(\theta) = \begin{cases} 0,\ for 0 < \theta < \theta_1, \theta_2 < \theta < \theta_3, \\ 1,\ for \theta_1 < \theta < \theta_2, \\ -1\, for \theta_3 < \theta < \theta\max \end{cases}$$

Where θ_1, θ_2, and θ_3 are radius of the first, second and the third zones, respectively. A MBCPF is positioned at the pupil plane, where the transmissions from the inner to the outer zone belts are 0, 1, 0, and-1 respectively. In this instance, we looked at the four belt CPF and the four angles that make up the set of four focus patterns that are optimized using the conventional global-search-optimization technique [26]. Utilizing this technique, we select a single structure with arbitrary values for θ1 through θ3 from all potential configurations and employ vector diffraction theory to model their focusing characteristics. During the optimization operations, the structure is selected as the initial structure if it generates a sub wavelength single focal spot and meets the limiting constraints that the Full With Half Maximum (FWHM) of the generated magnetization segment is less than 0.5.

3. RESULTS AND DISCUSSION

A detailed analysis of the magnetization distributions generated using an azimuthally polarized Laguerre-Bessel-Gaussian (LBG) beam modulated by a multi-belt complex phase filter (MBCPF). The numerical simulations used parameters: NA = 0.95, m = 1, λ = 1, and α = *arcsin* (NA). All lengths are normalized to λ, and the energy density is normalized to unity.

3.1. Two Magnetization Spot Segments

Figure 2(a) shows the magnetization distribution generated by the high NA lens and MBCPF optimized with specific angles. The result is two bright magnetization spots along the z-axis. The r-z plane field distribution reveals two distinct magnetization spots, each with sub-wavelength precision. As shown in Figure 2 (a), an array of two magnetization spot segments generated by the high NA lens and the MBCPF with θ_1 = 52.73°, θ_2 = 54.45°, θ_3 = 55.60°, θ_{max} = 71.65°, respectively. Here the magnetic two bright spots in the z direction. Figure 2(b) illustrates the longitudinal distribution of these spots. The Full Width Half Maximum (FWHM) of each spot is measured to be 0.27λ, and they are axially separated by 4λ. The depth of focus (DOF) for each spot is 2.5λ, highlighting the precision and confinement of the magnetization spots. This precise axial spacing ensures the magnetization spots do not interfere with each other, maintaining high resolution. Figure 2(c) shows the lateral distribution, confirming the sub-wavelength nature of the magnetization spots. The compact and precise magnetization distribution is ideal for applications requiring high spatial resolution, such as magnetic recording and particle trapping.

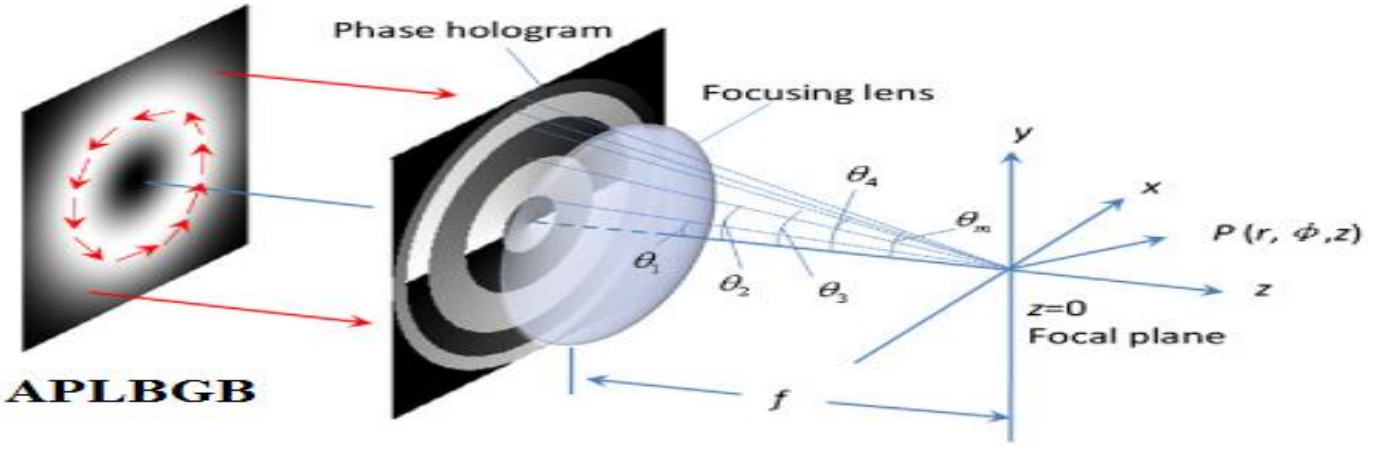

Fig. 1. Schematic setup to generate the sub-wavelength longitudinal magnetization chain for azimuthally polarized Laguerre–Bessel–Gaussian beam.

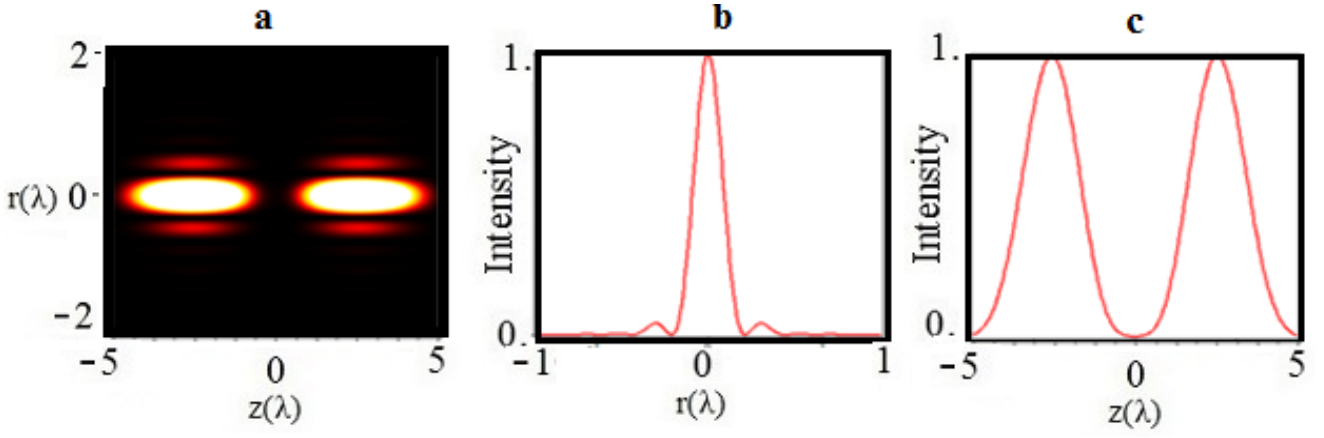

Fig. 2. Normalized magnetization distribution (a) through focus (r-z plane), (b) along the longitudinal direction, and (c) lateral direction.

3.2. Three Magnetization Spot Segments

Figure 3(a) presents an array of three sub-wavelength magnetization spots generated by another MBCPF configuration. The spots have a FWHM of 0.37λ and are axially separated by 1.76λ. This configuration demonstrates the ability to create multiple tightly focused magnetization spots, useful for applications requiring multi-point control. Figure 3(b) shows the longitudinal magnetization distribution, with each spot maintaining a consistent axial intensity. The DOF for each spot is measured to be 2.9λ, indicating a robust and stable magnetization chain. This stability is crucial for applications in precise magnetic manipulation. Figure 3(c) confirms the lateral distribution, illustrating the uniformity and sub-wavelength precision of the magnetization spots. The lateral confinement ensures that the spots can be used for high-density magnetic storage and multi-particle trapping without cross-talk between the spots.

3.3. Dual Trapping with Two Focal Spots

A set off angles of the MPCPF optimized to achieve the above mentioned task are θ_1 = 13.18°, θ_2 = 44.88°, θ_3 = 55.60°, θ_{max} = 71.65°, respectively. In order to achieve dual trapping, we suggested a MBSPH optimized with angles are θ_1 = 28.66°, θ_2 = 43.56°, θ_3 = 55.60°, and θ_{max} = 71.65°. These angles are optimized based on the above –mentioned method but with the limiting condition that the FWHM of the generated focal segment is less than 0.6 λ and there should be at least two such focal spots in the three focal segment. Figure 4(a) demonstrates the magnetization distribution for a different MBCPF configuration optimized to generate two sub-wavelength focal spots. Each spot has a FWHM of 0.31λ and a DOF of 1.23λ. The spots are axially separated by 1.1λ. This configuration is optimized for dual trapping, providing stable and precise trapping for particles.

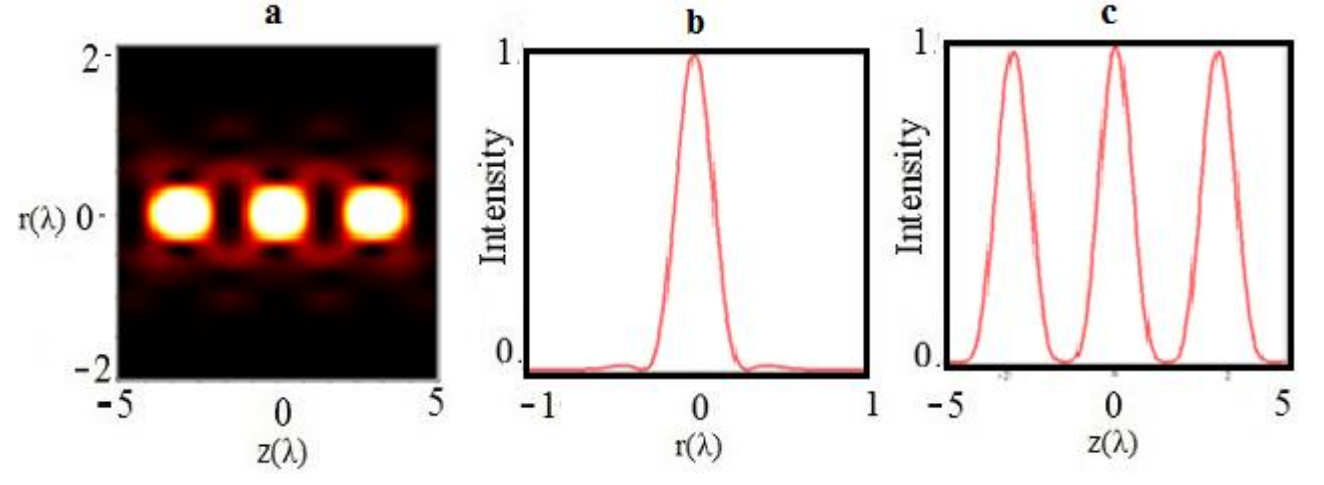

Fig. 3. Normalized magnetization distribution (a) through focus (r-z plane), (b) along the longitudinal direction, and (c) lateral direction.

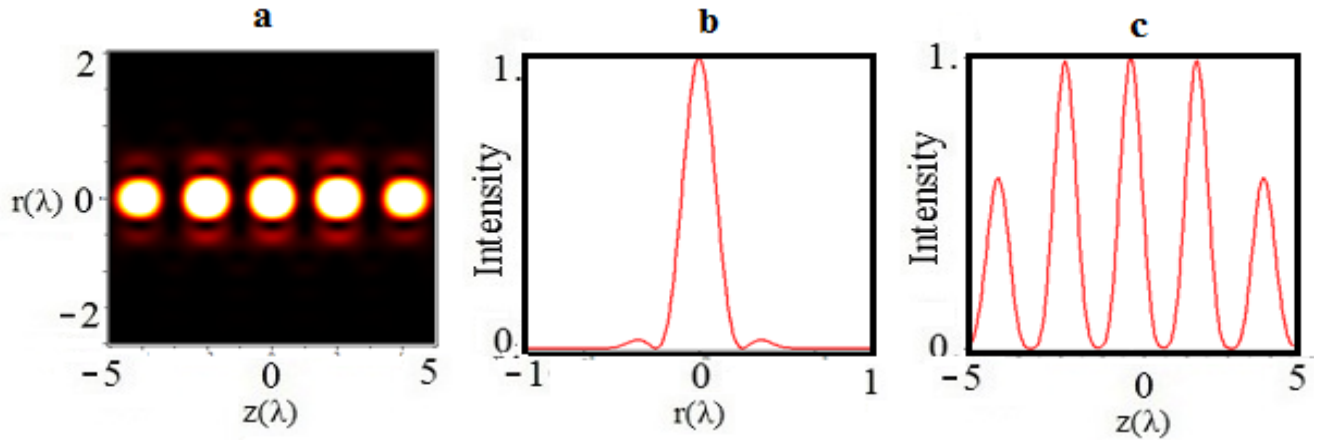

Fig. 4. Normalized magnetization distribution (a) through focus (r-z plane), (b) along the longitudinal direction, and (c) lateral direction.

Figure 4(b) shows the longitudinal distribution of the focal spots, confirming their precision and separation. The close spacing and stable DOF make this setup suitable for applications requiring precise control over two particles simultaneously, such as in quantum computing or high-precision measurements. Figure 4(c) illustrates the lateral distribution, indicating the stability and precision of the generated magnetization spots. The dual focal spots are ideal for applications requiring precise and stable trapping of particles with high refractive indices, such as in optical tweezers or nanofabrication.

3.4. Multiple Particle Trapping with Uniform Separation

Figure 5(a) shows the magnetization distribution generated by another MBCPF configuration, optimized to create uniformly separated focal spots. The array of two sub wavelength focal spots segment generated by the high NA lens for the MBSPH optimized with angles $\theta_1 = 11.46°$, $\theta_2 = 24.64°$, $\theta_3 = 55.65°$, and $\theta_{max} = 71.65°$, respectively. Each spot has a focal depth of around 1.2λ. The uniform separation ensures that each spot can be used independently without interference from adjacent spots. Figure 5(b) presents the longitudinal distribution, with each focal spot having a FWHM of 0.32λ and separated by 1.45λ. The consistent axial separation and uniform intensity of the spots highlight the effectiveness of the MBCPF in generating multiple focal spots. This setup is ideal for applications requiring precise control over multiple particles. Figure 5(c) confirms the lateral distribution, demonstrating the three-dimensional trapping capability of the focal spots. The engineered multiple focal spots can be used for multiple particle trapping, manipulation, delivery, and self-assembly. This precise control is crucial for advanced manufacturing processes and scientific research involving complex particle interactions.

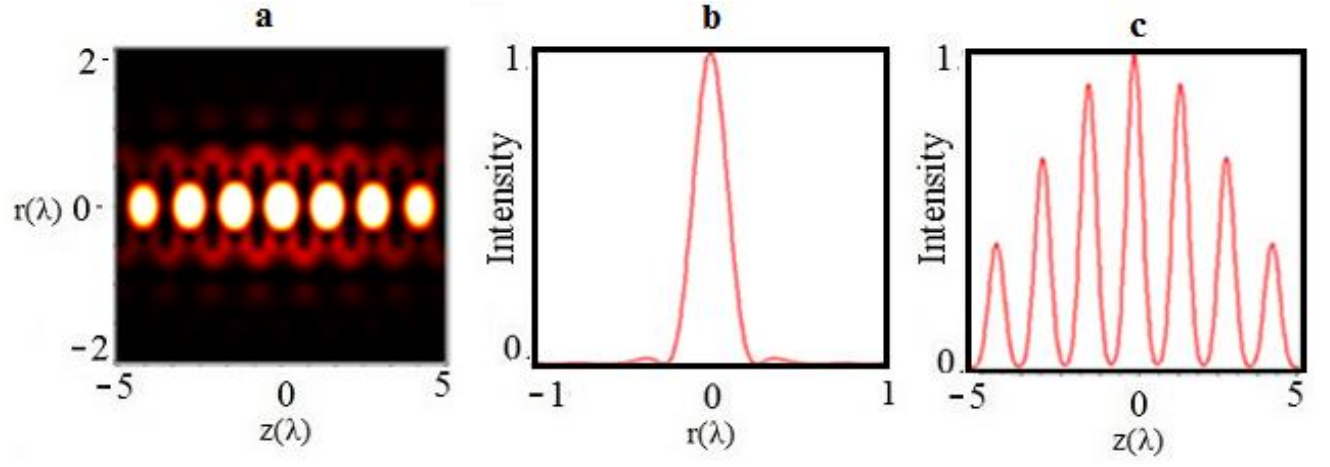

Fig. 5. Normalized magnetization distribution (a) through focus (r-z plane), (b) along the longitudinal direction, and (c) lateral direction.

The magnetization distributions generated by the azimuthally polarized LBG beam modulated by MBCPFs have been successfully demonstrated through numerical simulations. Each configuration showcased the ability to create precise and stable magnetization spots with sub-wavelength resolution. The results validate the potential of using such setups for high-resolution magnetic recording, precise particle trapping, and advanced optomagnetic applications. The successful application of the MBCPF configurations highlights their versatility and effectiveness in controlling magnetization distributions. The ability to generate multiple magnetization spots with precise control over their separation and intensity opens up new possibilities in various fields, including data storage, quantum computing, and biomedical applications. The findings underscore the potential of computationally optimized phase filters in advancing optomagnetic technologies and improving the performance of devices that rely on precise magnetization control.

4. CONCLUSION

In conclusion, the use of inverse Faraday effect (IFE) and vector diffraction theory has enabled the creation of light-induced longitudinal magnetization chains. By employing tightly focused Laguerre-Bessel-Gaussian beams with azimuthal polarization through a high numerical aperture focusing mechanism, we have successfully demonstrated a novel approach to study the total magnetization intensity distribution in the focal region. This research presents a new method to generate multiple magnetization spot segments at sub-wavelength scales by designing appropriate diffractive optical elements. The results showcase the potential of these configurations for various advanced applications, including multilayer magneto-optical data storage, ultra-compact optomagnetic devices, magnetic particle trapping and transportation, and the fabrication of magnetic lattices for spin wave operations. Additionally, the findings have significant implications for enhancing techniques in confocal and magnetic resonance microscopy. The proposed approach demonstrates the effectiveness and versatility of using azimuthally polarized Laguerre-Bessel-Gaussian beams in conjunction with complex phase filters, opening new avenues for precise and efficient manipulation of magnetization fields in various scientific and industrial applications.

CONFLICT OF INTEREST

The authors declare that there is no conflict of interests.

REFERENCES

[1] Albrecht, M., Rettner, C.T., Moser, A., Best, M.E. and Terris, B.D., **2002.** Recording performance of high-density patterned perpendicular magnetic media. *Applied Physics Letters*, *81*(15), pp.2875-2877.

[2] Stanciu, C.D., Hansteen, F., Kimel, A.V., Kirilyuk, A., Tsukamoto, A., Itoh, A. and Rasing, T., **2007.** All-optical magnetic recording with circularly polarized light. *Physical Review Letters*, *99*(4), p.047601.

[3] Khorsand, A.R., Savoini, M., Kirilyuk, A., Kimel, A.V., Tsukamoto, A., Itoh, A. and Rasing, T., **2012.** Role of magnetic circular dichroism in all-optical magnetic recording. *Physical Review Letters*, *108*(12), p.127205.

[4] Wang, S., Li, X., Zhou, J. and Gu, M., **2015.** All-optically configuring the inverse Faraday effect for nanoscale perpendicular magnetic recording. *Optics Express*, *23*(10), pp.13530-13536.

[5] Atutov, S.N., Calabrese, R., Guidi, V., Mai, B., Rudavets, A.G., Scansani, E., Tomassetti, L., Biancalana, V., Burchianti, A., Marinelli, C. and Mariotti, E., **2003.** Fast and efficient loading of a Rb magneto-optical trap using light-induced atomic desorption. *Physical Review A*, *67*(5), p.053401.

[6] Majors, P.D., Minard, K.R., Ackerman, E.J., Holtom, G.R., Hopkins, D.F., Parkinson, C.I., Weber, T.J. and Wind, R.A., **2002.** A combined confocal and magnetic resonance microscope for biological studies. *Review of Scientific Instruments*, *73*(12), pp.4329-4338.

[7] Grinolds, M.S., Warner, M., De Greve, K., Dovzhenko, Y., Thiel, L., Walsworth, R.L., Hong, S., Maletinsky, P. and Yacoby, A., **2014.** Subnanometre resolution in three-dimensional magnetic resonance imaging of individual dark spins. *Nature Nanotechnology*, *9*(4), pp.279-284.

[8] Zhang, Y., Okuno, Y. and Xu, X., **2009.** All-optical magnetic superresolution with binary pupil filters. *JOSA B*, *26*(7), pp.1379-1383.

[9] Zhang, Y. and Bai, J., **2008.** Theoretical study on all-optical magnetic recording using a solid immersion lens. *Journal of the Optical Society of America B*, *26*(1), pp.176-182.

[10] Li, X., Venugopalan, P., Ren, H., Hong, M. and Gu, M., **2014.** Super-resolved pure-transverse focal fields with an enhanced energy density through focus of an azimuthally polarized first-order vortex beam. *Optics Letters*, *39*(20), pp.5961-5964.

[11] Jiang, Y., Li, X. and Gu, M., **2013.** Generation of sub-diffraction-limited pure longitudinal magnetization by the inverse Faraday effect by tightly focusing an

azimuthally polarized vortex beam. *Optics Letters*, *38*(16), pp.2957-2960.

[12] Wang, S., Li, X., Zhou, J. and Gu, M., **2014.** Ultralong pure longitudinal magnetization needle induced by annular vortex binary optics. *Optics Letters*, *39*(17), pp.5022-5025.

[13] Ma, W., Zhang, D., Zhu, L. and Chen, J., **2015.** Super-long longitudinal magnetization needle generated by focusing an azimuthally polarized and phase-modulated beam. *Chinese Optics Letters*, *13*(5), pp.052101-052101.

[14] Nie, Z., Ding, W., Li, D., Zhang, X., Wang, Y. and Song, Y., **2015.** Spherical and sub-wavelength longitudinal magnetization generated by 4π tightly focusing radially polarized vortex beams. *Optics Express*, *23*(2), pp.690-701.

[15] Nie, Z., Ding, W., Shi, G., Li, D., Zhang, X., Wang, Y. and Song, Y., **2015.** Achievement and steering of light-induced sub-wavelength longitudinal magnetization chain. *Optics Express*, *23*(16), pp.21296-21305.

[16] Gong, L., Wang, L., Zhu, Z., Wang, X., Zhao, H. and Gu, B., **2016.** Generation and manipulation of super-resolution spherical magnetization chains. *Applied Optics*, *55*(21), pp.5783-5789.

[17] Richards, B. and Wolf, E., **1959.** Electromagnetic diffraction in optical systems, II. Structure of the image field in an aplanatic system. *Proceedings of the Royal Society of London. Series A. Mathematical and Physical Sciences*, *253*(1274), pp.358-379.

[18] Youngworth, K.S. and Brown, T.G., **2000.** Focusing of high numerical aperture cylindrical-vector beams. *Optics Express*, *7*(2), pp.77-87.

[19] Tovar, A.A., **2000.** Propagation of Laguerre–Bessel–Gaussian beams. *JOSA A*, *17*(11), pp.2010-2018.

[20] Mei, Z. and Zhao, D., **2007.** Nonparaxial analysis of vectorial Laguerre-Bessel-Gaussian beams. *Optics Express*, *15*(19), pp.11942-11951.

[21] Xu, Y., Singh, J., Sheppard, C.J. and Chen, N., **2007.** Ultra long high resolution beam by multi-zone rotationally symmetrical complex pupil filter. *Optics Express*, *15*(10), pp.6409-6413.

[22] Pershan, P.S., 1963. Nonlinear optical properties of solids: energy considerations. *Physical Review*, *130*(3), p.919.

[23] Van der Ziel, J.P., Pershan, P.S. and Malmstrom, L.D., 1965. Optically-induced magnetization resulting from the inverse Faraday effect. *Physical review letters*, *15*(5), p.190.

[24] Pershan, P.S., Van der Ziel, J.P. and Malmstrom, L.D., 1966. Theoretical discussion of the inverse Faraday effect, Raman scattering, and related phenomena. *Physical review*, *143*(2), p.574.

[25] Xu, Y., Singh, J., Sheppard, C.J. and Chen, N., 2007. Ultra long high resolution beam by multi-zone rotationally symmetrical complex pupil filter. *Optics Express*, *15*(10), pp.6409-6413.

[26] Zha, Y., Wei, J., Wang, H. and Gan, F., **2013.** Creation of an ultra-long depth of focus super-resolution longitudinally polarized beam with a ternary optical element. *Journal of Optics*, *15*(7), p.075703.